Research Article

Preventive electroacupuncture reduces cognitive deficits in a rat model of D-galactose-induced aging
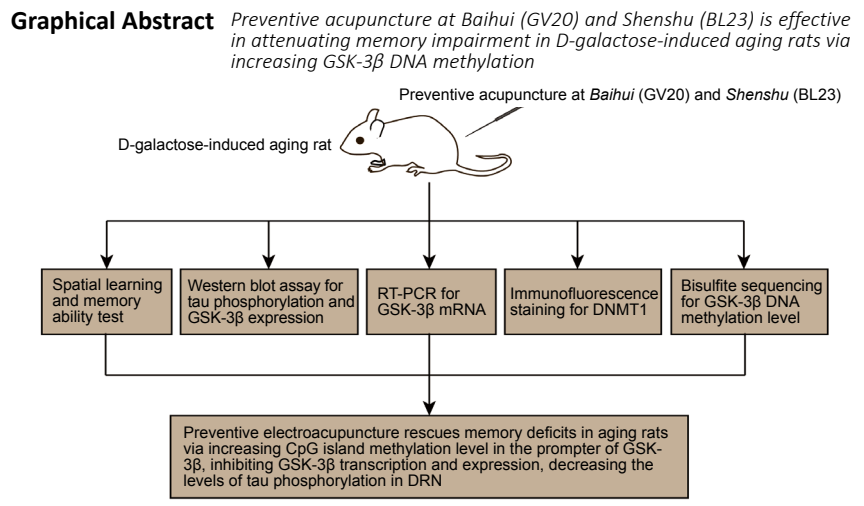
Chao-Chao Yu[1, 2, #], Chuan He[3, #], Yan-Jun Du[3], Shan Gao[4], Yuan-Fang Lin[1, 2], Shu-Qin Wang[1, 2], Li Wang[3], Jia Wang[4], Xue-Song Wang[3], Tao Jiang[3], Li-Hong Kong[3, *]

Graphical Abstract *Preventive acupuncture at Baihui (GV20) and Shenshu (BL23) is effective in attenuating memory impairment in D-galactose-induced aging rats via increasing GSK-3β DNA methylation*

Abstract

Acupuncture can reduce cognitive deficits in Alzheimer's disease. However, whether electroacupuncture can prevent or alleviate the cognitive deficits in animal models of aging remains poorly understood. Studies have shown that disordered epigenetic modifications play a critical role in age-related cognitive decline. Therefore, we hypothesized that preventive electroacupuncture might improve cognitive functions during aging by regulating epigenetic modifications. A rat model of aging was produced by intraperitoneal injection of 120 mg/kg D-galactose for 8 weeks. *Baihui* and *Shenshu* acupoints were stimulated by electroacupuncture for 8 weeks from the first day of D-galactose administration. Preventive electroacupuncture alleviated memory impairment, decreased tau hyperphosphorylation, and reduced glycogen synthase kinase-3β protein and mRNA expression levels in the brainstem dorsal raphe nucleus, where intracellular neurofibrillary tangle lesions first occur. In addition, the DNA methylation level in the promoter region of the glycogen synthase kinase-3β gene was increased. The effects of preventive electroacupuncture were stronger than those of preventive acupuncture. Intraperitoneal injection of 0.4 mg/kg 5-aza-2'-deoxycytidine, an inhibitor of DNA methyltransferase that blocks epigenetic modifications, antagonized the effects of preventive electroacupuncture. Our results suggest that preventive electroacupuncture treatment alleviates cognitive impairment in aging rats probably by affecting the epigenetic modification of the glycogen synthase kinase-3β gene in the dorsal raphe nucleus. This study was approved by the Animal Ethics Committee of Hubei University of Chinese Medicine, China (approval No. HUCMS201712001) on November 28, 2017.

Key Words: Alzheimer's disease; brain; central nervous system; cognitive impairment; DNA methylation; electroacupuncture; neurological function; pathways

Chinese Library Classification No. R454.1; R741; R339.3+8

Introduction

Alzheimer's disease (AD), a progressive neurodegenerative disorder, is the leading cause of dementia among older adults. It usually manifests clinically as progressive memory loss and executive dysfunction (McKhann et al., 2011; Zhao et al., 2016; Sumbria, 2020). As the worldwide population ages, it is estimated that nearly 1 million new cases per year globally will be expected by 2050, conferring a tremendous challenge on global healthcare systems (Alzheimer's Association, 2016). Extracellular amyloid-β (Aβ) plaques

[1]Department of Tuina, Shenzhen Traditional Chinese Medicine Hospital, Shenzhen, Guangdong Province, China; [2]The 4th Clinical College, Guangzhou University of Chinese Medicine, Shenzhen, Guangdong Province, China; [3]College of Acupuncture and Orthopedics, Hubei University of Chinese Medicine, Wuhan, Hubei Province, China; [4]Department of Acupuncture & Moxibustion, Wuhan Hospital of Integrated Chinese & Western Medicine, Tongji Medical College of Huazhong University of Science & Technology, Wuhan, Hubei Province, China
*Correspondence to: Li-Hong Kong, MD, xiyu1618@sina.com.
https://orcid.org/0000-0002-4287-0536 (Li-Hong Kong)
#Both authors contributed equally to this work.

and intracellular neurofibrillary tangles (NFTs), composed of hyperphosphorylated tau proteins, are the main pathological features of AD (Long and Holtzman, 2019). Though acetylcholinesterase inhibitors and the N-methyl-D-aspartate-type glutamate receptor antagonist memantine have been approved by the U.S. Food and Drug Administration for AD, their efficacy is modest and transient (Cummings, 2004). Because AD is insidious and difficult to reverse, it is important to develop effective prevention strategies.

The distribution pattern of NFTs resulting from tau hyperphosphorylation is highly predictable (Goedert et al., 2017), and it is the NFTs (Giannakopoulos et al., 2003), rather than senile plaques, that are associated with the severity of dementia. Considerable evidence suggests that NFT lesions first occur in the brainstem dorsal raphe nucleus (DRN) (Grinberg et al., 2009; Simic et al., 2009), and NFT-associated lesions in the DRN can even be observed in presymptomatic stages (Rüb et al., 2000). The DRN contains long projection neurons that are abundant in serotonin. These neurons project to several brain areas associated with cognitive function, such as the frontal cortex, hippocampus, septum, striatum and amygdala (Hornung, 2003). In addition, the early occurrence of non-cognitive and behavioral symptoms in prodromal AD, such as depression and general disturbances in mood (Chen et al., 2000; Wu et al., 2003), suggests the involvement of the DRN in AD. Hyperphosphorylation of tau protein leads to its aggregation into paired helical filament-like structures, which are the major constituents of NFTs (Šimić et al., 2016). Therefore, it is reasonable to speculate that early inhibition of tau hyperphosphorylation could have therapeutic potential for preventing and treating AD. Glycogen synthase kinase-3β (GSK-3β) is a serine/threonine protein kinase that is the main protein kinase that phosphorylates tau. It has been demonstrated that tau hyperphosphorylation caused by GSK-3β overexpression and activation results in perturbed synaptic morphologies and impaired synaptic transmission (Hu et al., 2015; Zhu et al., 2018).

Aging is the primary risk factor for AD (Hou et al., 2019). Disordered epigenetic modifications are associated with age-related cognitive decline in AD (Lardenoije et al., 2015; Nativio et al., 2018). Epigenetic changes, including DNA methylation, histone modification and regulation by non-coding RNAs, refer to heritable alterations in gene expression that are independent of DNA sequence (Holliday, 1994). Accumulating evidence indicates that abnormal DNA methylation could contribute to the pathogenesis of AD and lead to cognitive dysfunction (Qazi et al., 2018). Aβ deposition, tau hyperphosphorylation (Mano et al., 2017) and neuroinflammation (Nicolia et al., 2017b) accompanied by altered DNA methylation levels have been observed in both AD patients (Coppieters et al., 2014) and AD mouse models (Chouliaras et al., 2018; Lardenoije et al., 2018). Epigenetic-directed therapy could be a potential approach for AD (Wood, 2018). Decreased cytosine methylation levels in the promoter region can induce the transcription of AD-related genes (Fuso, 2013; Cui et al., 2018; Qazi et al., 2018). DNA methylation of cytosine results in the formation of 5-methylcytosine, and is mediated by DNA methyltransferase (DNMT) (Siegfried and Simon, 2010). DNMT1 is considered a maintenance DNMT, and its function is to copy the existing methylation pattern during the repair and replication of DNA (Lyko, 2018). Accumulating evidence indicates that DNMT1 levels are altered in AD patients (Mastroeni et al., 2010; Chouliaras et al., 2013). Epigenetic modifications can directly or indirectly regulate tau phosphorylation, thereby impacting AD development and progression. It was reported recently that treatment with a DNA demethylating agent significantly upregulates GSK-3β mRNA in murine mesenchymal stem cells (Cho et al., 2009). S-adenosylmethionine is the main methyl donor in the DNA methylation process and is synthesized by one-carbon metabolism (Siegfried and Simon, 2010). A previous study showed that one-carbon metabolism changes caused by B-vitamin deficiency upregulates GSK-3β mRNA (Nicolia et al., 2010). Therefore, we hypothesized that DNA methylation might regulate GSK-3β gene expression. DNMT1 is a key enzyme regulating DNA methylation level and gene transcription (Cui and Xu, 2018). A recent postmortem study found hypomethylated CpG islands, and associated GSK-3β mRNA overexpression and increased GSK-3β activity, in patients with initial AD, suggesting that GSK-3β hyperactivity as a result of altered DNMT activity could promote NFT formation in the early stages of AD (Nicolia et al., 2017a). Thus, DNMT could be a promising target for drug discovery in AD (Cacabelos and Torrellas, 2014; Cui and Xu, 2018).

Clinical trials indicate that acupuncture is effective and safe for AD (Jia et al., 2017; Feng et al., 2019). Additionally, accumulating experimental evidence suggests that acupuncture can ameliorate cognitive dysfunction in transgenic AD mice by reducing senile plaque burden (Tang et al., 2019), attenuating neuroinflammation (Cai et al., 2019), prompting hippocampal neurogenesis (Li et al., 2014), and enhancing hippocampal glucose metabolism (Cao et al., 2017). But whether acupuncture can prevent or alleviate cognitive impairments in animal models of aging remains unclear. Our previous study showed that 50 Hz electroacupuncture (EA) rescues hippocampal synaptic injuries and memory deficits in the transgenic Aβ$_{1-42}$ AD rat model probably by inhibiting GSK-3β (Yu et al., 2018). Furthermore, it was reported that inhibition of GSK-3β and p38 is involved in the EA-mediated reduction of the streptozotocin-induced increase in tau phosphorylation (Rocco et al., 2013). Herein, we investigate whether preventive EA (PEA) can prevent and ameliorate cognitive decline in aging rats by reducing GSK-3β expression and tau hyperphosphorylation in the DRN.

Materials and Methods

Animals
Seventy-two specific-pathogen-free adult male Sprague-Dawley rats, approximately aged three months and weighing 330 ± 20 g, were purchased from the Laboratory Animal Center of China Three Gorges University, China (license No. SCXK (E) 2017-0012). Rats were acclimated for a week prior to the experiment. All rats were housed (n = 4 per cage) at 20 ± 2°C and a relative humidity of 50 ± 10% under a 12-hour light/dark cycle (lights on at 8:00 a.m.), with free access to food and water. The rats were randomly divided into the following six groups (n = 12 per group) using a random number table: control, model (D-galactose; D-gal), PEA + inhibitor (D-gal + PEA + inhibitor), inhibitor (D-gal + inhibitor), preventive manual acupuncture (D-gal + PMA), and PEA (D-gal + PEA). All animal procedures were approved by the Animal Ethics Committee of Hubei University of Chinese Medicine, Wuhan, China (approval No. HUCMS201712001) on November 28, 2017.

Intervention
Rats in the model, PEA + inhibitor, inhibitor, PMA and PEA groups were injected with D-gal (Sinopharm, Shanghai, China) intraperitoneally daily (120 mg/kg per day) for 8 weeks (Hong et al., 2016). Rats in the control group received no D-gal injection.

EA treatment was performed as described in our previous study (Yu et al., 2018). During PEA + inhibitor and PEA treatment, rats were wrapped with tailored and soft cloth materials in the prone position in a conscious state rather than anesthetized. Starting on the first day of intraperitoneal injection of D-gal, PEA was administered at Baihui (GV20; 15° obliquely to a depth of 3–5 mm at the center of the parietal bone, and the needle was inserted into the epicranial aponeurosis) and alternating unilateral Shenshu

(BL23; perpendicularly to a 3–5 mm depth adjacent to the second lumbar vertebra) to rats in the PEA + inhibitor and PEA groups once daily for 8 consecutive weeks (**Additional Figure 1**). In the PMA group, twirling manipulation was applied every 5 minutes for 10 seconds. Each needle was rotated bidirectionally 90° at a speed of 90°/s. No twirling manipulation was applied in the PEA group. EA was delivered using stainless steel needles (15 mm in length and 0.3 mm in diameter; Beijing Zhongyan Taihe Medical Apparatus Co., Ltd., Beijing, China) and an EA apparatus (HANS-100A; Beijing Huayun Ante Science and Technology Co., Ltd., Beijing, China). At GV20, the needle was inserted 15° obliquely to a depth of 3–5 mm. At BL23, the needle was inserted perpendicularly to a depth of 3–5 mm. In our previous studies (Wang et al., 2017; Yu et al., 2018), EA at a frequency of 50 Hz showed a stronger protective effect in transgenic $A\beta_{1-42}$ rats. Accordingly, stimulation at a continuous wave at 50 Hz was applied to the PEA + inhibitor and PEA groups for 20 minutes each day at the pair of acupuncture points (GV20 and alternating unilateral BL23). The intensity (1 mA) was adjusted to induce light muscle contractions. In the PMA group, GV20 and BL23 points were stimulated, but the needles were not connected to current.

At the beginning of week 7, rats in the PEA + inhibitor and inhibitor groups were injected intraperitoneally with 5-aza-2′-deoxycytidine, an inhibitor of DNMT, daily (0.4 mg/kg per day) for a week (Pereira et al., 2004; Sales et al., 2011). Rats in the control and model groups were wrapped in the same way but received no other intervention.

Morris water maze test

The Morris water maze test was performed after the interventions as described in our previous study (Yu et al., 2018). The apparatus (Chengdu Taimeng Technology Co., Ltd., Chengdu, China) consisted of a large circular pool (120 cm in diameter, 50 cm in height) and a MT-200 Morris water maze video-tracking system (Chengdu Taimeng Technology Co., Ltd.). The pool was filled with water (24 ± 2°C), made opaque with milk, to a depth of 40 cm, and divided into four equal quadrants (**Additional Figure 2**). The circular platform (10 cm in diameter) was placed at the midpoint of the target quadrant and submerged approximately 1.5 cm below the surface of the water. All rats were trained for 5 consecutive days in standard place-navigation trials. Rats were placed in a quadrant facing the wall of the pool on four occasions (every time in different quadrants). The rats were given no more than 120 seconds to find the hidden platform in each trial, and the time was recorded as the escape latency. When the rat failed to find the platform within this period, it was assisted onto the platform and allowed to remain there for 10 seconds. The rats rested for 30 seconds between trials. For the spatial probe trial (conducted the next day after the place navigation test), the platform was removed from the pool. This test was performed in the same manner as the place navigation test. The rats were given 120 seconds to swim in the pool. The time spent in the target quadrant (the quadrant where the hidden platform was located during training trials) was recorded. The data and swimming path were recorded using Watermaze 2.0 software (Chengdu Taimeng Technology Co., Ltd.).

Western blot assay

After the behavioral tests were completed, the rats were sacrificed for molecular biological tests. Western blot assay was performed as described in a previous study (Szőnyi et al., 2019). Six rats from each group were randomly selected for western blot assay. DRN tissues were immediately separated, and lysates were prepared as previously described. Equal amounts of protein from each sample were separated by Tris-glycine sodium dodecyl sulfate–polyacrylamide gel electrophoresis and transferred onto nitrocellulose membranes (Millipore, Billerica, MA, USA) electrophoretically.

After blocking with 5% non-fat dry milk in Tris-buffered saline with 0.1% Tween-20 for 1 hour at room temperature, the membranes were incubated overnight at 4°C with the following primary antibodies: GSK-3β (mouse; 1:800; Cat# ab93926; Abcam, Inc., Cambridge, MA, USA), GSK-3β-pTyr216 (rabbit; 1:900; Cat# ab75745; Abcam, Inc.), GSK-3β-pSer9 (rabbit; 1:800; Cat# 5558T; Cell Signaling Technology, Danvers, MA, USA), tau-5 (mouse; 1 µg/mL; Cat# ab80579; Abcam, Inc.), paired helical filament 1 (PHF-1; rabbit; 1:1000; Cat# ab184951; Abcam, Inc.), tau-pS262 (rabbit; 1:600; Cat# ab131354; Abcam, Inc.). After washes, the membranes were incubated with horseradish peroxidase-conjugated affinipure goat anti-mouse IgG (H+L) (goat; 1:3000; Cat# SA00001-2; Proteintech Inc., Wuhan, China) or horseradish peroxidase-conjugated affinipure goat anti-mouse IgG (H+L) (goat; 1:2000; Cat# SA00001-1; Proteintech Inc.) at 37°C for 1 hour. A chemiluminescence detection system (ChemiDoc XRS+, Bio-Rad, Hercules, CA, USA) was used to measure the protein signals. All western blot data were quantified with Image-Pro Plus 6 software (National Institutes of Health, Bethesda, MD, USA). Normalization was performed by blotting the same membranes with glyceraldehyde-3-phosphate dehydrogenase (GAPDH; rabbit; 1:400; Cat# A00227-1; Boster, Wuhan, China), and confirmed by triplicate measurements of the same sample.

Immunofluorescence staining

Another three rats in each group were randomly selected for immunofluorescence staining. Rats were deeply anesthetized with 10% chloral hydrate (400 mg/kg) and transcardially perfused with normal saline, followed by 4% paraformaldehyde in 0.1 M phosphate buffer (pH 7.4, 4°C). The brains were then quickly extracted and post fixed in 4% paraformaldehyde in 0.1 M phosphate buffer for 4 hours. The tissue blocks containing the DRN were dehydrated and embedded in paraffin. Brain paraffin sections (about 5 µm) in the coronal plane containing the DRN were processed with a standard antigen retrieval procedure, and blocked for 1 hour with 10% goat serum. Then, sections were incubated with DNMT1 primary antibody (rabbit; 1 µg/mL; Cat# ab188453; Abcam, Inc.) at 37°C for 1 hour and at 4°C overnight. Subsequently, brain sections were washed with phosphate-buffered saline and incubated at 37 °C for 1 hour with the secondary antibody (IgG H&L; goat; 1:700; Cat# ab6939; Abcam, Inc.) labeled with Cy3. Nuclei were stained with 4′,6-diamino-2-phenylindole. Images were acquired using a laser confocal fluorescence microscope (TCS SP8; Leica, Mannheim, Germany). For the negative control, primary antibody was replaced with phosphate-buffered saline. Three sections from each group were randomly selected for analysis. DNMT1-positive neurons (optical density of the fluorescence exceeding background by 50%) in the DRN were counted at 400× magnification, and the relative number of immunoreactive cells was calculated as the ratio of positive neurons to total neurons (by counting 4′,6-diamino-2-phenylindole-stained nuclei).

Real-time polymerase chain reaction

Remaining fresh brain tissues after the western blot assay were used for real-time polymerase chain reaction (PCR). Three rats from each group were randomly selected for real-time-PCR assay. RNA from the DRN was extracted with the Easyspin plus tissue/cell RNA kit (Cat# RN2802; Aidlab Biotech, Beijing, China). An aliquot (1 µg) of extracted RNA was used to synthesize complementary DNA using a ReverTra Ace qPCR RT kit (FSK-101; Toyobo, Shanghai, China). The primer sequences were the following: GSK-3β: 5′-ATC TTT GGA GCC ACC GAT TAC-3′, 5′-TTG CTC CCT TGT TGG TGT TC-3′; GAPDH: 5′-CGC TAA CAT CAA ATG GGG TG-3′, 5′-TTG CTG ACA ATC TTG AGG GAG-3′. Primers were obtained from HY Cell Biotechnology Co., Ltd. (Wuhan, China). Complementary

DNA level was quantified using an EnTurbo™ SYBR Green PCR SuperMix (Car#EQ001; ELK Biotechnology, Wuhan, China). Thermocycling was performed on a StepOne Real-Time PCR System (Life Technologies, Carlsbad, CA, USA). Measurements were conducted in triplicate and normalized to the GAPDH control. The fold change in relative mRNA level was determined using the $2^{-\Delta\Delta Ct}$ method.

DNA methylation analysis by bisulfite sequencing

GSK-3β gene promoter methylation was analyzed by bisulfite sequencing. DNA samples were prepared from the DRN, and then purified and processed for bisulfite modification with the EZ Methylation-Gold Kit (Cat#D5005; ZYMO Research, Orange County, CA, USA). A fragment of ~328 bp in the GSK-3β promoter region was amplified. The primers used for bisulfite analysis were the following: 5′-TGG AGT TGT TTA GTT AAT GAG GAA A-3′, 5′-ACC TAA ACT AAA ACC AAT CAA AAA C-3′. The obtained PCR products were then ligated into the pDrive cloning vector with a PCR cloning kit. The ligation products were cloned, and 10 clones for each experimental condition were analyzed. Sequencing of the purified plasmid DNA was performed by Genecreate Biological Engineering Co., Ltd. (Wuhan, China) using a DNA analyzer (ABI 3730xl DNA Analyzer; Applied Biosystems, Waltham, MA, USA). The obtained data packages were uploaded to the online Quantification tool for Methylation Analysis (http://quma.cdb.riken.jp/) to analyze the methylation percentage of each CpG site.

Statistical analysis

Data were tested for normal distribution using the Kolmogorov-Smirnov test. Normally distributed data were expressed as the mean ± standard deviation (SD) and analyzed using GraphPad Prism 6.0 for Windows (GraphPad Software, San Diego, CA, USA). Statistical significance was determined by one-way analysis of variance followed by the least significant difference test. A level of $P < 0.05$ was considered statistically significant.

Results

PEA effectively improves spatial learning and memory in the rat model of D-gal-induced aging

As shown in **Figure 1**, rats given intraperitoneal injection of D-gal showed impaired learning and memory abilities, as evidenced by the increased escape latency to find the hidden platform in the navigation trial. Compared with the model group, the escape latency was significantly increased in the inhibitor group from day 3 ($P < 0.01$), but was decreased in the PEA + inhibitor ($P < 0.01$), PEA ($P < 0.01$) and PMA groups ($P < 0.01$). Furthermore, escape latency was shorter in the PEA group than in the PMA ($P < 0.01$) and PEA + inhibitor ($P < 0.01$) groups. Memory deficit was also assessed by removing the hidden platform in the spatial probe trial. Compared with the model group, the time spent in the target quadrant was significantly decreased in the inhibitor group ($P < 0.01$), but was increased in the PEA + inhibitor ($P < 0.01$), PEA ($P < 0.01$) and PMA groups ($P < 0.01$). In addition, the target quadrant times were significantly longer in the PMA ($P < 0.01$) and PEA + inhibitor ($P < 0.01$) groups compared with the model group. These results indicate that PEA and PMA treatments both rescue the learning and memory impairments in the rat model of D-gal-induced aging, and that PEA has a stronger protective effect.

PEA significantly decreases the levels of phosphorylated tau in the DRN in the rat model of D-gal-induced aging

Intraperitoneal injection with D-gal increased tau-5, PHF-1 and tau-pS262 levels in the DRN compared with the control group ($P < 0.01$). Compared with the model group, the expression of tau-5, PHF-1 and tau-pS262 were significantly decreased
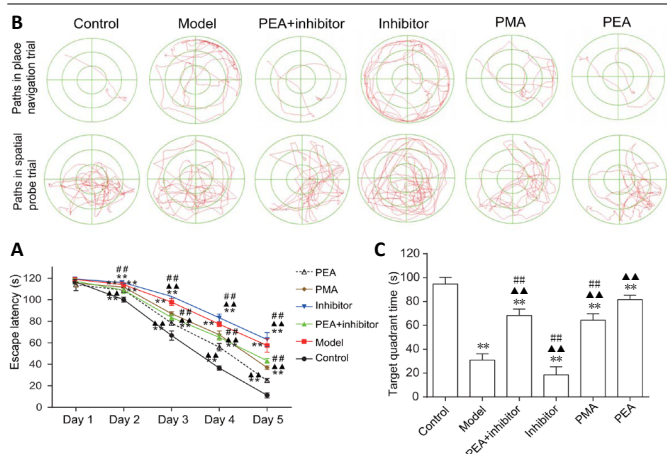
in the PEA + inhibitor, PMA and PEA groups ($P < 0.01$), but no statistically significant difference was observed between the model and inhibitor groups ($P > 0.05$). The expression levels of tau-5 ($P < 0.01$) and tau-pS262 ($P < 0.05$) were lower in the PEA group than in the PMA group (**Figure 2**). These results indicate that PMA and PEA treatments reduce the levels of total tau (tau-5), PHF-1 and tau-pS262.

PEA and PMA inhibit GSK-3β in the DRN in the rat model of D-gal-induced aging

To investigate the mechanism underlying D-gal-induced tau hyperphosphorylation, western blotting was performed to detect the expression levels of GSK-3β and to assess its activation state. As shown in **Figure 3**, increased GSK-3β activity, as evidenced by elevated levels of GSK-3β and GSK-3β-pTyr216, and decreased levels of GSK-3β-pSer9 were observed in the DRN after intraperitoneal injection of D-gal, suggesting that GSK-3β activity is upregulated in the DRN in rats with D-gal-induced aging. Compared with the model group, the levels of total GSK-3β and GSK-3β-pTyr216 were significantly decreased in rats in the PEA + inhibition, PMA and PEA groups ($P < 0.01$), while no statistically significant difference was observed between the inhibitor and model groups ($P > 0.05$). The level of inactive GSK-3β-pSer9 in the inhibitor group was reduced compared with the model group ($P < 0.01$). Furthermore, the levels of GSK-3β-pSer9 in the PMA and PEA groups were increased compared with the model group ($P < 0.01$). Unexpectedly, no significant differences were detected between the model and PEA + inhibitor groups, but the level of GSK-3β-pSer9 was higher in the PEA group compared with the PEA + inhibitor and inhibitor groups ($P < 0.01$). No statistically significant difference in total GSK-3β, GSK-3β-pTyr216 or GSK-3β-pSer9 was observed between the PMA and PEA groups ($P > 0.05$). These results indicate that PMA and PEA treatments both inhibit the activity of GSK-3β, thereby decreasing tau phosphorylation levels in the DRN in the rat model of D-gal-induced aging.
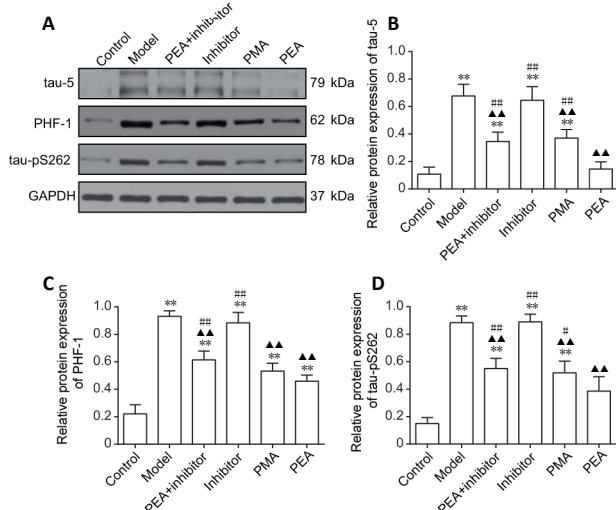
PEA and PMA increase GSK-3β gene promoter methylation levels and decrease GSK-3β mRNA expression in the DRN in the rat model of D-gal-induced aging

In the present study, we observed that the DNMT inhibitor 5-aza-2′-deoxycytidine aggravated memory dysfunction, synaptic damage and tau hyperphosphorylation, and that PEA treatment ameliorated the synaptic morphological changes and restored cognitive function, suggesting that modulation of DNA methylation might be involved in the neuroprotective effect of PEA. Therefore, we next studied the levels of cytosine methylation in the promoter region of the GSK-3β gene in the DRN (**Figure 4A**). As shown in **Figure 4C**, intraperitoneal injection of D-gal decreased the methylation level in the CpG islands of the GSK-3β gene promoter, and upregulated the expression of GSK-3β mRNA in the DRN. Compared with the model group, the cytosine methylation level in the gene promoter in the inhibitor group was decreased ($P < 0.05$), but was increased in the PEA + inhibitor ($P < 0.05$), PMA ($P < 0.05$) and PEA groups ($P < 0.01$). No statistically significant difference was observed between the PMA and PEA groups ($P > 0.05$). As shown in **Figure 4B**, compared with the model group, GSK-3β mRNA expression was increased in the inhibitor group ($P < 0.05$), but was decreased in the PEA + inhibitor ($P < 0.01$), PMA ($P < 0.01$) and PEA groups ($P < 0.01$). Unexpectedly, GSK-3β mRNA level in the PEA group was higher than that in the PMA group ($P < 0.01$), suggesting that other epigenetic modulatory pathways could also be involved in the PEA-induced silencing of the GSK-3β gene. These findings indicate that PEA and PMA treatments inhibit the transcription of the GSK-3β gene in the DRN, in turn decreasing tau phosphorylation levels, in the rat model of D-gal-induced aging.
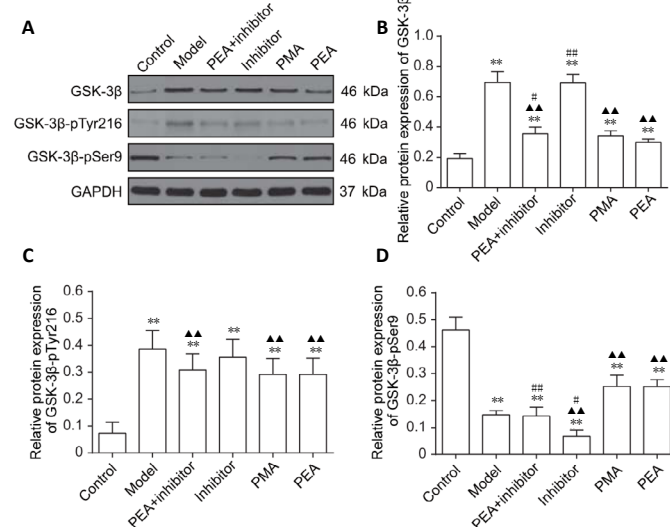
Figure 2 │ Effects of acupuncture treatment on the expression of phosphorylated tau in the dorsal raphe nucleus in the rat model of D-galactose-induced aging.
(A) The protein expression levels of tau-5, PHF-1 and tau-pS262 in the dorsal raphe nucleus were detected using western blot assay. GAPDH was used as a loading control. (B–D) Quantitative results for tau-5 (B), PHF-1 (C) and tau-pS262 (D) expression (optical density ratio to GAPDH). The data are expressed as the mean ± SD ($n = 6$). **$P < 0.01$, *vs.* control group; ▲▲$P < 0.01$, *vs.* model group; #$P < 0.05$, ##$P < 0.01$, *vs.* PEA group (one-way analysis of variance followed by the least significant difference test). Control: Normal; Model: D-galactose-induced aging; PEA + inhibitor: D-galactose-induced aging + preventive electroacupuncture + 5-aza-2′-deoxycytidine (an inhibitor of DNA methyltransferase); Inhibitor: D-galactose-induced aging + 5-aza-2′-deoxycytidine; PMA: D-galactose-induced aging + preventive manual acupuncture; PEA: D-galactose-induced aging + preventive electroacupuncture. GAPDH: glyceraldehyde-3-phosphate dehydrogenase; PHF-1: paired helical filament 1.

Figure 3 │ Effects of acupuncture treatment on the expression of GSK-3β in the dorsal raphe nucleus in the rat model of D-galactose-induced aging.
(A) The protein levels of total GSK-3β, GSK-3β-pTyr216 and GSK-3β-pSer9 in the dorsal raphe nucleus were detected by western blot assay. GAPDH was used as a loading control. (B–D) Quantitative results for GSK-3β (B), GSK-3β-pTyr216 (C) and GSK-3β-pSer9 (D) levels. The data are expressed as the mean ± SD ($n = 6$). **$P < 0.01$, *vs.* control group; ▲▲$P < 0.01$, *vs.* model group; #$P < 0.05$, ##$P < 0.01$, *vs.* PEA group (one-way analysis of variance followed by the least significant difference test). Control: Normal; Model: D-galactose-induced aging; PEA + inhibitor: D-galactose-induced aging + preventive electroacupuncture + 5-aza-2′-deoxycytidine (an inhibitor of DNA methyltransferase); Inhibitor: D-galactose-induced aging + 5-aza-2′-deoxycytidine; PMA: D-galactose-induced aging + preventive manual acupuncture; PEA: D-galactose-induced aging + preventive electroacupuncture. GAPDH: glyceraldehyde-3-phosphate dehydrogenase; GSK-3β: glycogen synthase kinase-3β.

PEA and PMA increase the expression of DNMT1 in the DRN in the rat model of D-gal-induced aging

Next, we studied the expression of DNMT1 in the DRN in rats with D-gal-induced aging. As shown in **Figure 5**, the expression of DNMT1 in the DRN was significantly decreased in the rat model of D-gal-induced aging. Compared with the model group, the expression of DNMT1 in the inhibitor group was decreased ($P < 0.05$ in immunofluorescence staining, $P < 0.05$ in western blot assay), but increased in the PEA + inhibitor ($P < 0.01$ in immunofluorescence staining, $P < 0.05$ in western blot assay), PMA ($P < 0.01$ in immunofluorescence staining, $P < 0.05$ in western blot) and PEA groups ($P < 0.01$ in immunofluorescence staining, $P < 0.05$ in western blot). In addition, the expression levels of DNMT1 were decreased in the PEA + inhibitor ($P < 0.01$ in immunofluorescence staining, $P < 0.01$ in western blot assay), inhibitor ($P < 0.01$ in immunofluorescence staining, $P < 0.01$ in western blot) and

PMA groups ($P < 0.05$ in immunofluorescence staining, $P < 0.05$ in western blot assay) compared with the PEA group. These results indicate that PEA increases GSK-3β DNA methylation levels by upregulating the expression of DNMT1, and that PEA is more effective than PMA.

Discussion

It is well documented that NFTs in the DRN are an early pathological feature in AD (Grinberg et al., 2009), and that epigenetic dysregulation participates in the pathogenesis of age-related cognitive disorders such as AD (Lardenoije et al., 2015). In the present study, we investigated the effects of PEA and PMA on tau phosphorylation and learning and memory functions in a D-gal-induced aging rat model, which is known to exhibit cognitive impairment and AD-like pathologies, including Aβ deposition (Tsai et al., 2011), tau hyperphosphorylation (Hong et al., 2016), neuroinflammation
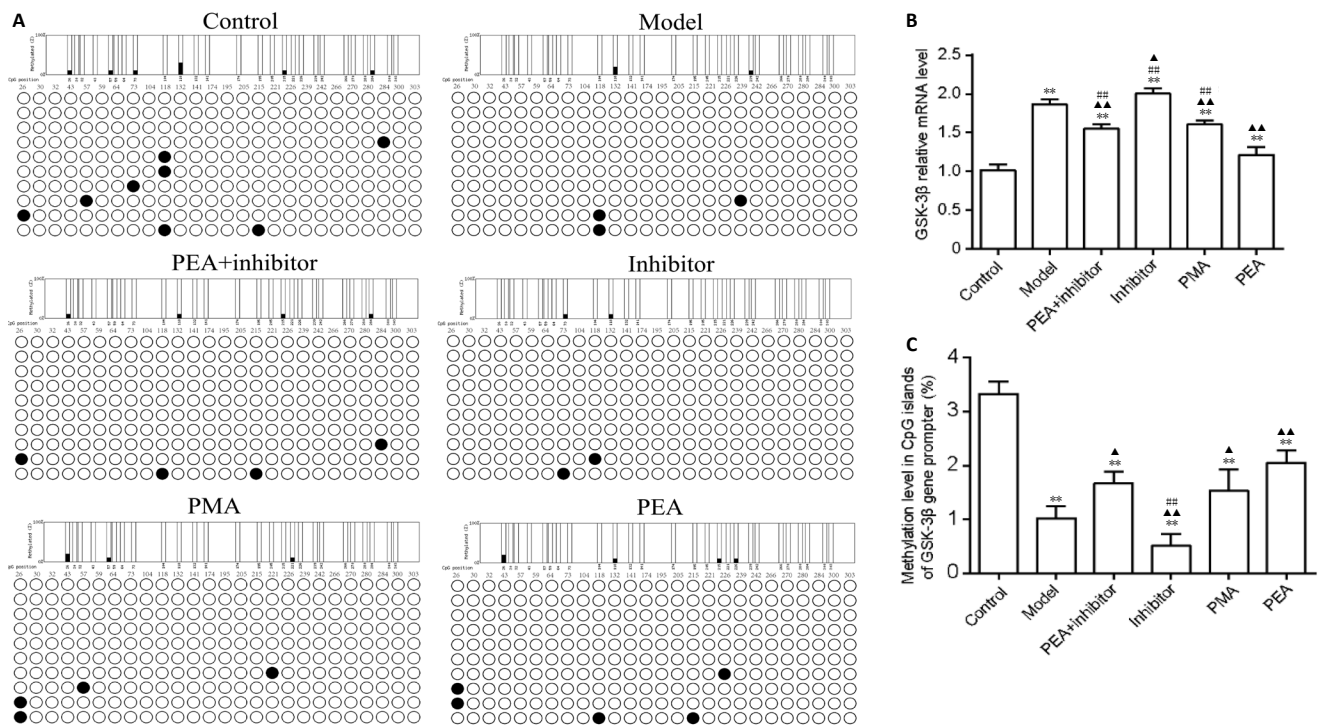
Figure 4 | Effects of acupuncture treatment on cytosine methylation in the promoter region of the GSK-3β gene and GSK-3β mRNA levels in the dorsal raphe nucleus in the rat model of D-galactose-induced aging.

(A) The methylation level in the promoter region of GSK-3β was detected using bisulfite sequencing-polymerase chain reaction. (B) Quantitation of GSK-3β mRNA levels, detected using real-time polymerase chain reaction. (C) Quantitation of methylation levels in CpG islands of the GSK-3β gene promoter. The data are expressed as the mean ± SD ($n = 3$). $**P < 0.01$, *vs.* control group; $▲P < 0.05$, $▲▲P < 0.01$, *vs.* model group; $\#\#P < 0.01$, *vs.* PEA group (one-way analysis of variance followed by the least significant difference test). Control: Normal; Model: D-galactose-induced aging; PEA + inhibitor: D-galactose-induced aging + preventive electroacupuncture + 5-aza-2′-deoxycytidine; Inhibitor: D-galactose-induced aging + 5-aza-2′-deoxycytidine; PMA: D-galactose-induced aging + preventive manual acupuncture; PEA: D-galactose-induced aging + preventive electroacupuncture. GAPDH: glyceraldehyde-3-phosphate dehydrogenase; GSK-3β: glycogen synthase kinase-3β.
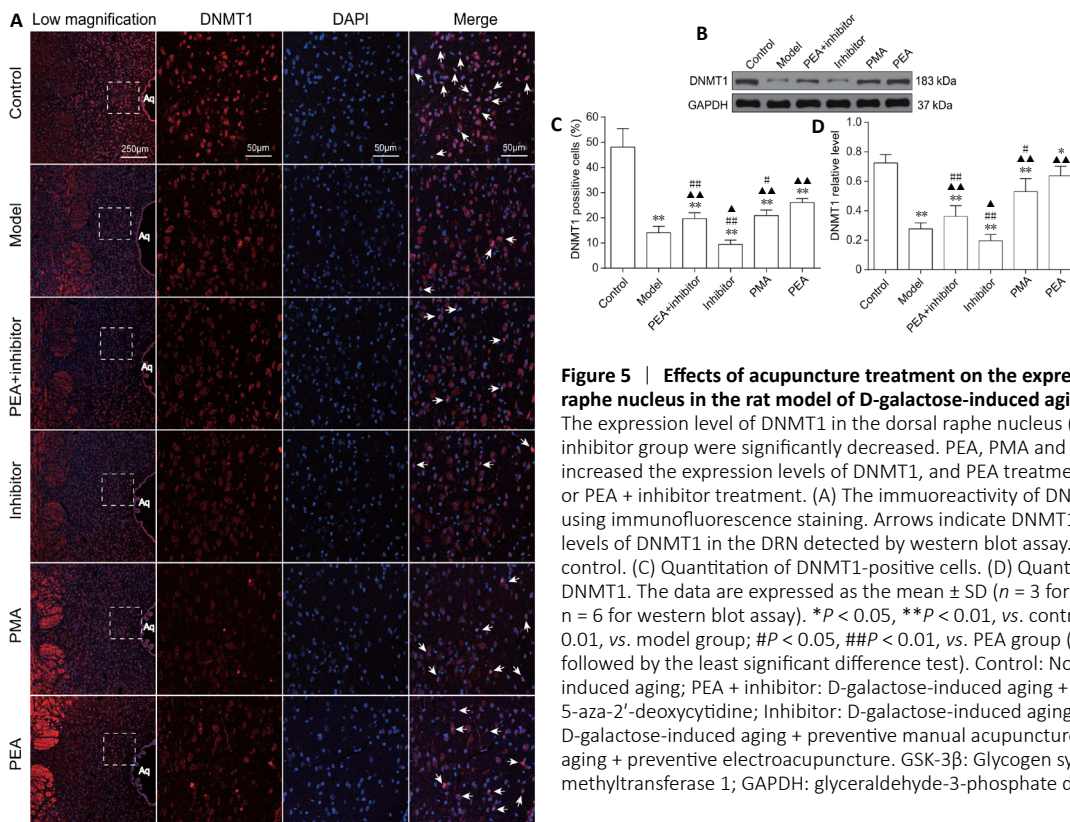
Figure 5 | Effects of acupuncture treatment on the expression of DNMT1 in the dorsal raphe nucleus in the rat model of D-galactose-induced aging.

The expression level of DNMT1 in the dorsal raphe nucleus (DRN) in the model group and inhibitor group were significantly decreased. PEA, PMA and PEA + inhibitor treatments all increased the expression levels of DNMT1, and PEA treatment was more effective than PMA or PEA + inhibitor treatment. (A) The immuoreactivity of DNMT1 in the DRN was detected using immunofluorescence staining. Arrows indicate DNMT1-positive cells. (B) The protein levels of DNMT1 in the DRN detected by western blot assay. GAPDH was used as a loading control. (C) Quantitation of DNMT1-positive cells. (D) Quantitation of protein expression of DNMT1. The data are expressed as the mean ± SD ($n = 3$ for immunofluorescence staining, n = 6 for western blot assay). $*P < 0.05$, $**P < 0.01$, *vs.* control group; $▲P < 0.05$, $▲▲P < 0.01$, *vs.* model group; $\#P < 0.05$, $\#\#P < 0.01$, *vs.* PEA group (one-way analysis of variance followed by the least significant difference test). Control: Normal; Model: D-galactose-induced aging; PEA + inhibitor: D-galactose-induced aging + preventive electroacupuncture + 5-aza-2′-deoxycytidine; Inhibitor: D-galactose-induced aging + 5-aza-2′-deoxycytidine; PMA: D-galactose-induced aging + preventive manual acupuncture; PEA: D-galactose-induced aging + preventive electroacupuncture. GSK-3β: Glycogen synthase kinase-3β; DNMT1: DNA methyltransferase 1; GAPDH: glyceraldehyde-3-phosphate dehydrogenase.

Research Article

(Gao et al., 2016) and cholinergic deficits (Zhang et al., 2014). In the current study, we found that chronic intraperitoneal injection of D-gal induced significant spatial learning and memory impairment, consistent with previous studies (Zhan et al., 2014; Fu et al., 2018). In addition, we observed elevated hyperphosphorylated tau proteins, decreased GSK-3β DNA methylation, as well as increased GSK-3β activity in the DRN. Notably, we demonstrated that PEA increased cytosine methylation of the GSK-3β gene promoter region by increasing the expression of DNMT1, thereby attenuating GSK-3β-mediated tau hyperphosphorylation. This is the first study to our knowledge to investigate the effects of acupuncture treatment on aging animals from the perspective of epigenetics.

Our findings confirm the key role of GSK-3β in tau phosphorylation (Hernandez et al., 2013). The activity of GSK-3β is inhibited by phosphorylation at Ser9 and activated by phosphorylation at Tyr216 (Hernandez et al., 2013). GSK-3β activity is strongly correlated with synaptic plasticity and memory (Jaworski et al., 2019). Tau hyperphosphorylation as a result of increased GSK-3β activity can cause a reduction in synapse-associated proteins and dendritic morphological damage (Hu et al., 2015; Zhu et al., 2018). In the present study, we found that GSK-3β and tau phosphorylation were upregulated in the DRN in rats with D-gal-induced aging, consistent with previous studies (Hong et al., 2016). We observed that PEA decreased the levels of phosphorylated tau in the DRN by inhibiting GSK-3β. It has been reported that EA can decrease tau phosphorylation levels and ameliorate cognitive impairments in diabetic rats by inhibiting GSK-3β (Rocco et al., 2013). Interestingly, though PEA and PMA treatment showed equivalent inhibitory effects on GSK-3β, tau phosphorylation levels were lower in PEA-treated rats than in PMA-treated animals, suggesting other proteins or signaling pathways associated with tau phosphorylation could also be impacted by PEA. Previous studies reported that EA decreases the levels of phosphorylated tau by regulating several signaling pathways, including the p38 mitogen-activated protein kinase pathway (Zhang et al., 2015; Wang et al., 2018), cyclic adenosine monophosphate/protein kinase A/ cyclic adenosine monophosphate-response element binding protein pathway (Yi et al., 2014), c-Jun N-terminal kinase and ERK1/2 (Wang et al., 2018).

Mounting evidence suggests that NFTs appear earlier in the DRN than other brain regions. It has been reported that NFTs in the DRN can propagate to highly vulnerable subcortical areas (Rüb et al., 2000; Grinberg et al., 2009; Simic et al., 2009), such as the entorhinal cortex, hippocampus and neocortex (Parvizi et al., 2001; Grinberg et al., 2009; Rodríguez et al., 2012). Once released, intracellular tau aggregates extracellularly and spreads transneuronally to interconnected brain areas, such as the hippocampus and cortex, thereby inducing the production of abnormal tau in those regions (Mirbaha et al., 2015). The mechanisms underlying the transneuronal spread of NFTs to other interconnected brain regions and the role of the DRN–hippocampus neural circuit in AD remains unclear. A recent study demonstrated that neurons in the median raphe expressing vesicular glutamate transporter 2 project to both the lateral habenula and medial ventral tegmental area, and activation of these neurons induces depression-related anhedonia and fear memory acquisition (Szőnyi et al., 2019). Also, it was reported that vesicular glutamate transporter 2 neurons in the median raphe facilitate long-term memory formation related to negative experience (Cui et al., 2018; Yang et al., 2018).

In the current study, we observed that both PEA and PMA increased DNMT1 levels in the DRN, but that PEA was more effective in increasing the expression of DNMT1 than PMA. Unexpectedly, though both PEA and PMA increased the methylation level of CpG sites in the GSK-3β gene promoter,

no significant difference was observed between PEA and PMA. However, PEA showed stronger inhibitory effects on GSK-3β transcription as evidenced by lower GSK-3β mRNA levels. This suggests that other epigenetic modifications could be involved in the PEA-mediated inhibition, which can be further investigated using miRNA array and chromatin immunoprecipitation sequencing analysis. Additionally, PEA plus inhibitor treatment improved learning and memory functions. Their combined effect was weaker than PEA, but stronger than inhibitor alone, suggesting that the inhibitor did not completely block the effects of PEA. These results indicate that other effector pathways are also involved in the neuroprotective effects of PEA. There is mounting evidence of the beneficial effects of acupuncture in AD, as discussed in previous reviews (Cao et al., 2016; Tu et al., 2019; Yu et al., 2019). Evidence from neuroimaging studies indicates that EA can induce a wide brain response associated with cognitive processing and memory, including the prefrontal cortex (Ghafoor et al., 2019) and hippocampus (Tan et al., 2017). Functional connectivity between the hippocampus and the precentral gyrus, which is significantly compromised in AD patients, can also be enhanced by acupuncture treatment (Zheng et al., 2018). Inhibition of the c-Jun N-terminal kinase signal transduction pathway has also been implicated in acupuncture-induced Alzheimer precursor protein downregulation (Tang et al., 2020). Ding et al. (2019) found that acupuncture rescued the cognitive dysfunction in SAMP8 mice by inhibiting the astrocytic phospholipase A2–arachidonic acid pathway, resulting in increased cerebral blood flow in the prefrontal lobe and hippocampus. These lines of evidence suggest that the beneficial effects of acupuncture in AD is achieved via the modulation of multiple targets and pathways.

There are several limitations to the present study. DNMT1 is a key DNMT that is crucial for the maintenance of DNA methylation state. A decreased DNMT1 level implies an increase in DNA hypomethylation (Chouliaras et al., 2013). Here, we only tested the methylation level of CpG islands in the GSK-3β gene promoter without consideration of other genes associated with tau phosphorylation, such as cyclin-dependent kinase 5 or protein phosphatase 2A (Šimić et al., 2016). Analysis of cyclin-dependent kinase 5 and protein phosphatase 2A DNA methylation states should be performed in future studies. In addition, we only investigated the effects of acupuncture treatment in the rat model of D-gal-induced aging, and the effects of acupuncture should be evaluated in other aging models, such as SAMP8 mice with AD traits.

In conclusion, we found in the present study that PEA increases the methylation levels of CpG islands in the GSK-3β gene promoter, leading to decreased GSK-3β transcription and expression and decreased tau phosphorylation in the DRN. In addition, PEA was more effective than PMA in alleviating cognitive dysfunction in rats with D-gal-induced aging. Our findings may help advance the development of new prevention strategies for AD. We will analyze dendritic ultrastructural morphological changes in the brain of rats with D-galactose-induced aging after EA intervention in future studies. This will provide insight into whether EA can mitigate ultrastructural changes caused by galactose.

Author contributions: *Study design and manuscript writing: CCY, CH; data analysis: SG, JW, SQW; experimental implementation: TJ, XSW, LW; study guidance: YJD; manuscript revision: LHK, YJD, YFL. All authors approved the final version of the manuscript.*

References

Alzheimer's Association (2016) 2016 Alzheimer's disease facts and figures. Alzheimers Dement 12:459-509.

Cacabelos R, Torrellas C (2014) Epigenetic drug discovery for Alzheimer's disease. Expert Opin Drug Discov 9:1059-1086.

Cai M, Lee JH, Yang EJ (2019) Electroacupuncture attenuates cognition impairment via anti-neuroinflammation in an Alzheimer's disease animal model. J Neuroinflammation 16:264.

Cao J, Tang Y, Li Y, Gao K, Shi X, Li Z (2017) Behavioral changes and hippocampus glucose metabolism in APP/PS1 transgenic mice via electro-acupuncture at governor vessel acupoints. Front Aging Neurosci 9:5.

Cao Y, Zhang LW, Wang J, Du SQ, Xiao LY, Tu JF, Liu CZ (2016) Mechanisms of acupuncture effect on Alzheimer's disease in animal-based researches. Curr Top Med Chem 16:574-578.

Chen CP, Eastwood SL, Hope T, McDonald B, Francis PT, Esiri MM (2000) Immunocytochemical study of the dorsal and median raphe nuclei in patients with Alzheimer's disease prospectively assessed for behavioural changes. Neuropathol Appl Neurobiol 26:347-355.

Cho J, Rameshwar P, Sadoshima J (2009) Distinct roles of glycogen synthase kinase (GSK)-3alpha and GSK-3beta in mediating cardiomyocyte differentiation in murine bone marrow-derived mesenchymal stem cells. J Biol Chem 284:36647-36658.

Chouliaras L, Mastroeni D, Delvaux E, Grover A, Kenis G, Hof PR, Steinbusch HW, Coleman PD, Rutten BP, van den Hove DL (2013) Consistent decrease in global DNA methylation and hydroxymethylation in the hippocampus of Alzheimer's disease patients. Neurobiol Aging 34:2091-2099.

Chouliaras L, Lardenoije R, Kenis G, Mastroeni D, Hof PR, van Os J, Steinbusch HWM, van Leeuwen FW, Rutten BPF, van den Hove DLA (2018) Age-related Disturbances in DNA (hydroxy)methylation in APP/PS1 Mice. Transl Neurosci 9:190-202.

Coppieters N, Dieriks BV, Lill C, Faull RL, Curtis MA, Dragunow M (2014) Global changes in DNA methylation and hydroxymethylation in Alzheimer's disease human brain. Neurobiol Aging 35:1334-1344.

Cui D, Xu X (2018) DNA methyltransferases, DNA methylation, and age-associated cognitive function. Int J Mol Sci 19:1315.

Cui Y, Yang Y, Ni Z, Dong Y, Cai G, Foncelle A, Ma S, Sang K, Tang S, Li Y, Shen Y, Berry H, Wu S, Hu H (2018) Astroglial Kir4.1 in the lateral habenula drives neuronal bursts in depression. Nature 554:323-327.

Cummings JL (2004) Alzheimer's disease. N Engl J Med 351:56-67.

Ding N, Jiang J, Tian H, Wang S, Li Z (2019) Benign regulation of the astrocytic phospholipase A(2)-arachidonic acid pathway: the underlying mechanism of the beneficial effects of manual acupuncture on CBF. Front Neurosci 13:1354.

Feng Q, Bin LL, Zhai YB, Xu M, Liu ZS, Peng WN (2019) Long-term efficacy and safety of electroacupuncture on improving MMSE in patients with Alzheimer's disease. Zhongguo Zhen Jiu 39:3-8.

Fu P, Zhang Q, Yi DY, Abdelmaksoud A, Huang Q, Zhao HY, Xiang W, Xiong NX (2018) Dehydrocavidine attenuates d-galactose induced learning and memory impairment in rats. Neurosci Lett 665:200-205.

Fuso A (2013) The 'golden age' of DNA methylation in neurodegenerative diseases. Clin Chem Lab Med 51:523-534.

Gao J, Zhou R, You X, Luo F, He H, Chang X, Zhu L, Ding X, Yan T (2016) Salidroside suppresses inflammation in a D-galactose-induced rat model of Alzheimer's disease via SIRT1/NF-κB pathway. Metab Brain Dis 31:771-778.

Ghafoor U, Lee JH, Hong KS, Park SS, Kim J, Yoo HR (2019) Effects of acupuncture therapy on MCI patients using functional near-infrared spectroscopy. Front Aging Neurosci 11:237.

Giannakopoulos P, Herrmann FR, Bussière T, Bouras C, Kövari E, Perl DP, Morrison JH, Gold G, Hof PR (2003) Tangle and neuron numbers, but not amyloid load, predict cognitive status in Alzheimer's disease. Neurology 60:1495-1500.

Goedert M, Eisenberg DS, Crowther RA (2017) Propagation of tau aggregates and neurodegeneration. Annu Rev Neurosci 40:189-210.

Grinberg LT, Rüb U, Ferretti RE, Nitrini R, Farfel JM, Polichiso L, Gierga K, Jacob-Filho W, Heinsen H (2009) The dorsal raphe nucleus shows phospho-tau neurofibrillary changes before the transentorhinal region in Alzheimer's disease. A precocious onset? Neuropathol Appl Neurobiol 35:406-416.

Hernandez F, Lucas JJ, Avila J (2013) GSK3 and tau: two convergence points in Alzheimer's disease. J Alzheimers Dis 33 Suppl 1:S141-144.

Holliday R (1994) Epigenetics: an overview. Dev Genet 15:453-457.

Hong XP, Chen T, Yin NN, Han YM, Yuan F, Duan YJ, Shen F, Zhang YH, Chen ZB (2016) Puerarin ameliorates D-galactose induced enhanced hippocampal neurogenesis and tau hyperphosphorylation in rat brain. J Alzheimers Dis 51:605-617.

Hornung JP (2003) The human raphe nuclei and the serotonergic system. J Chem Neuroanat 26:331-343.

Hou Y, Dan X, Babbar M, Wei Y, Hasselbalch SG, Croteau DL, Bohr VA (2019) Ageing as a risk factor for neurodegenerative disease. Nat Rev Neurol 15:565-581.

Hu J, Huang HZ, Wang X, Xie AJ, Wang X, Liu D, Wang JZ, Zhu LQ (2015) Activation of glycogen synthase kinase-3 mediates the olfactory deficit-induced hippocampal impairments. Mol Neurobiol 52:1601-1617.

Jaworski T, Banach-Kasper E, Gralec K (2019) GSK-3β at the intersection of neuronal plasticity and neurodegeneration. Neural Plast 2019:4209475.

Jia Y, Zhang X, Yu J, Han J, Yu T, Shi J, Zhao L, Nie K (2017) Acupuncture for patients with mild to moderate Alzheimer's disease: a randomized controlled trial. BMC Complement Altern Med 17:556.

Lardenoije R, van den Hove DLA, Havermans M, van Casteren A, Le KX, Palmour R, Lemere CA, Rutten BPF (2018) Age-related epigenetic changes in hippocampal subregions of four animal models of Alzheimer's disease. Mol Cell Neurosci 86:1-15.

Lardenoije R, Iatrou A, Kenis G, Kompotis K, Steinbusch HW, Mastroeni D, Coleman P, Lemere CA, Hof PR, van den Hove DL, Rutten BP (2015) The epigenetics of aging and neurodegeneration. Prog Neurobiol 131:21-64.

Li X, Guo F, Zhang Q, Huo T, Liu L, Wei H, Xiong L, Wang Q (2014) Electroacupuncture decreases cognitive impairment and promotes neurogenesis in the APP/PS1 transgenic mice. BMC Complement Altern Med 14:37.

Long JM, Holtzman DM (2019) Alzheimer disease: an update on pathobiology and treatment strategies. Cell 179:312-339.

Lyko F (2018) The DNA methyltransferase family: a versatile toolkit for epigenetic regulation. Nat Rev Genet 19:81-92.

Mano T, Nagata K, Nonaka T, Tarutani A, Imamura T, Hashimoto T, Bannai T, Koshi-Mano K, Tsuchida T, Ohtomo R, Takahashi-Fujigasaki J, Yamashita S, Ohyagi Y, Yamasaki R, Tsuji S, Tamaoka A, Ikeuchi T, Saido TC, Iwatsubo T, Ushijima T, et al. (2017) Neuron-specific methylome analysis reveals epigenetic regulation and tau-related dysfunction of BRCA1 in Alzheimer's disease. Proc Natl Acad Sci U S A 114:E9645-9654.

Mastroeni D, Grover A, Delvaux E, Whiteside C, Coleman PD, Rogers J (2010) Epigenetic changes in Alzheimer's disease: decrements in DNA methylation. Neurobiol Aging 31:2025-2037.

McKhann GM, Knopman DS, Chertkow H, Hyman BT, Jack CR, Jr., Kawas CH, Klunk WE, Koroshetz WJ, Manly JJ, Mayeux R, Mohs RC, Morris JC, Rossor MN, Scheltens P, Carrillo MC, Thies B, Weintraub S, Phelps CH (2011) The diagnosis of dementia due to Alzheimer's disease: recommendations from the National Institute on Aging-Alzheimer's Association workgroups on diagnostic guidelines for Alzheimer's disease. Alzheimers Dement 7:263-269.

Mirbaha H, Holmes BB, Sanders DW, Bieschke J, Diamond MI (2015) Tau trimers are the minimal propagation unit spontaneously internalized to seed intracellular aggregation. J Biol Chem 290:14893-14903.

Nativio R, Donahue G, Berson A, Lan Y, Amlie-Wolf A, Tuzer F, Toledo JB, Gosai SJ, Gregory BD, Torres C, Trojanowski JQ, Wang LS, Johnson FB, Bonini NM, Berger SL (2018) Dysregulation of the epigenetic landscape of normal aging in Alzheimer's disease. Nat Neurosci 21:497-505.

Nicolia V, Fuso A, Cavallaro RA, Di Luzio A, Scarpa S (2010) B vitamin deficiency promotes tau phosphorylation through regulation of GSK3beta and PP2A. J Alzheimers Dis 19:895-907.

Nicolia V, Ciraci V, Cavallaro RA, Ferrer I, Scarpa S, Fuso A (2017a) GSK3β 5'-flanking DNA methylation and expression in Alzheimer's disease patients. Curr Alzheimer Res 14:753-759.

Nicolia V, Cavallaro RA, López-González I, Maccarrone M, Scarpa S, Ferrer I, Fuso A (2017b) DNA methylation profiles of selected pro-inflammatory cytokines in Alzheimer disease. J Neuropathol Exp Neurol 76:27-31.

Parvizi J, Van Hoesen GW, Damasio A (2001) The selective vulnerability of brainstem nuclei to Alzheimer's disease. Ann Neurol 49:53-66.

Pereira MA, Wang W, Kramer PM, Tao L (2004) DNA hypomethylation induced by non-genotoxic carcinogens in mouse and rat colon. Cancer Lett 212:145-151.

Qazi TJ, Quan Z, Mir A, Qing H (2018) Epigenetics in Alzheimer's disease: perspective of DNA methylation. Mol Neurobiol 55:1026-1044.

Rocco ML, Pristerà A, Pistillo L, Aloe L, Canu N, Manni L (2013) Brain cholinergic markers and Tau phosphorylation are altered in experimental type 1 diabetes: normalization by electroacupuncture. J Alzheimers Dis 33:767-773.

Rodríguez JJ, Noristani HN, Verkhratsky A (2012) The serotonergic system in ageing and Alzheimer's disease. Prog Neurobiol 99:15-41.

Rüb U, Del Tredici K, Schultz C, Thal DR, Braak E, Braak H (2000) The evolution of Alzheimer's disease-related cytoskeletal pathology in the human raphe nuclei. Neuropathol Appl Neurobiol 26:553-567.

Sales AJ, Biojone C, Terceti MS, Guimarães FS, Gomes MV, Joca SR (2011) Antidepressant-like effect induced by systemic and intra-hippocampal administration of DNA methylation inhibitors. Br J Pharmacol 164:1711-1721.

Siegfried Z, Simon I (2010) DNA methylation and gene expression. Wiley Interdiscip Rev Syst Biol Med 2:362-371.

Simic G, Stanic G, Mladinov M, Jovanov-Milosevic N, Kostovic I, Hof PR (2009) Does Alzheimer's disease begin in the brainstem? Neuropathol Appl Neurobiol 35:532-554.

Šimić G, Babić Leko M, Wray S, Harrington C, Delalle I, Jovanov-Milošević N, Bažadona D, Buée L, de Silva R, Di Giovanni G, Wischik C, Hof PR (2016) Tau protein hyperphosphorylation and aggregation in Alzheimer's disease and other tauopathies, and possible neuroprotective strategies. Biomolecules 6:6.

Sumbria RK (2020) Targeting the transferrin receptor to develop erythropoietin for Alzheimer's disease. Neural Regen Res 15:2251-2252.

Szőnyi A, Zichó K, Barth AM, Gönczi RT, Schlingloff D, Török B, Sipos E, Major A, Bardóczi Z, Sos KE, Gulyás AI, Varga V, Zelena D, Freund TF, Nyiri G (2019) Median raphe controls acquisition of negative experience in the mouse. Science 366:eaay8746.

Tan TT, Wang D, Huang JK, Zhou XM, Yuan X, Liang JP, Yin L, Xie HL, Jia XY, Shi J, Wang F, Yang HB, Chen SJ (2017) Modulatory effects of acupuncture on brain networks in mild cognitive impairment patients. Neural Regen Res 12:250-258.

Tang Y, Xu A, Shao S, Zhou Y, Xiong B, Li Z (2020) Electroacupuncture ameliorates cognitive impairment by inhibiting the JNK signaling pathway in a mouse model of Alzheimer's disease. Front Aging Neurosci 12:23.

Tang Y, Shao S, Guo Y, Zhou Y, Cao J, Xu A, Wu J, Li Z, Xiang D (2019) Electroacupuncture mitigates hippocampal cognitive impairments by reducing BACE1 deposition and activating PKA in APP/PS1 double transgenic mice. Neural Plast 2019:2823679.

Tsai SJ, Chiu CP, Yang HT, Yin MC (2011) s-Allyl cysteine, s-ethyl cysteine, and s-propyl cysteine alleviate β-amyloid, glycative, and oxidative injury in brain of mice treated by D-galactose. J Agric Food Chem 59:6319-6326.

Tu CH, MacDonald I, Chen YH (2019) The effects of acupuncture on glutamatergic neurotransmission in depression, anxiety, schizophrenia, and Alzheimer's disease: a review of the literature. Front Psychiatry 10:14.

Wang Y, Liu ZB, Niu WM, Wang Q (2018) Influence of Xiusanzhen on cognition and protein expression of Aβ and phosphorylated JNK, ERK1/2 in hippocampus of mice with Alzheimer's disease. Nanjing Zhongyiyao Daxue Xuebao 34:376-380.

Wang Y, Kong L, Li W, Zhang K, Shen F, Wang Y, Zhou H, Sun G (2017) Effects and mechanisms of different frequencies of electroacupuncture for learning and memory ability of Alzheimer's rats. Zhongguo Zhen Jiu 37:629-636.

Wood IC (2018) The contribution and therapeutic potential of epigenetic modifications in Alzheimer's disease. Front Neurosci 12:649.

Wu YH, Feenstra MG, Zhou JN, Liu RY, Toranõ JS, Van Kan HJ, Fischer DF, Ravid R, Swaab DF (2003) Molecular changes underlying reduced pineal melatonin levels in Alzheimer disease: alterations in preclinical and clinical stages. J Clin Endocrinol Metab 88:5898-5906.

Yang Y, Cui Y, Sang K, Dong Y, Ni Z, Ma S, Hu H (2018) Ketamine blocks bursting in the lateral habenula to rapidly relieve depression. Nature 554:317-322.

Yi XF, Peng L, Zhang ZY, Xiao M, Mu JP, Xie LY, Chen XS, Gao X, Liang PF (2014) Influence of electroacupuncture on cAMP/PKA/CREB signal transduction pathways in Aβ25-35 induced Alzheimer's disease model rats. Zhonghua Shiyong Zhenduan yu Zhiliao Zazhi 28:128-130.

Yu CC, Wang Y, Shen F, Kong LH, Wang YW, Zhou H, Tang L (2018) High-frequency (50 Hz) electroacupuncture ameliorates cognitive impairment in rats with amyloid beta 1-42-induced Alzheimer's disease. Neural Regen Res 13:1833-1841.

Yu CC, Ma CY, Wang H, Kong LH, Zhao Y, Shen F, Wu M (2019) Effects of acupuncture on Alzheimer's disease: evidence from neuroimaging studies. Chin J Integr Med 25:631-640.

Zhan PY, Peng CX, Zhang LH (2014) Berberine rescues D-galactose-induced synaptic/memory impairment by regulating the levels of Arc. Pharmacol Biochem Behav 117:47-51.

Zhang M, Xu GH, Wang WX, Luo CF, Lu RZ, Meng DJ (2015) Study of electro-acupuncture on phosphorylation of tau protein in Alzheimer's disease rats through p38MAPK signaling pathway. Nanjing Zhongyiyao Daxue Xuebao 31:261-264.

Zhang R, Zhang J, Fang L, Li X, Zhao Y, Shi W, An L (2014) Neuroprotective effects of sulforaphane on cholinergic neurons in mice with Alzheimer's disease-like lesions. Int J Mol Sci 15:14396-14410.

Zhao H (2016) Embryonic neural stem cell transplantation for Alzheimer's disease. Embryonic neural stem cell transplantation for Alzheimer's disease. Zhongguo Zuzhi Gongcheng Yanjiu 20:4805-4810.

Zheng W, Su Z, Liu X, Zhang H, Han Y, Song H, Lu J, Li K, Wang Z (2018) Modulation of functional activity and connectivity by acupuncture in patients with Alzheimer disease as measured by resting-state fMRI. PLoS One 13:e0196933.

Zhu H, Zhang W, Zhao Y, Shu X, Wang W, Wang D, Yang Y, Yang Y, He Z, Wang X, Ying Y (2018) GSK3β-mediated tau hyperphosphorylation triggers diabetic retinal neurodegeneration by disrupting synaptic and mitochondrial functions. Mol Neurodegener 13:62.

C-Editor: Zhao M; S-Editors: Yu J, Li CH; L-Editors: Patel B, Yu J, Song LP; T-Editor: Jia Y
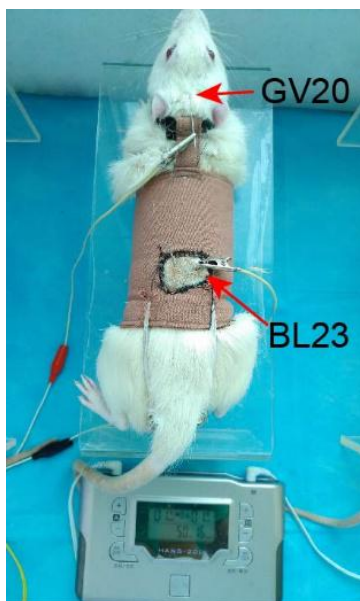
Additional Figure 1 Rats receiving acupuncture treatment.

BL23: *Shenshu*; GV20: *Baihui*.

Additional Figure 2 Morris water maze test.

The pool was filled with opaque water.